Scramjet Performance Achieved in Engine Tests from M4 to M8 Flight Conditions

Tohru Mitani(1), Sadatake Tomioka(1), Takeshi Kanda(1), Nobuo Chinzei(1)
and Toshinori Kouchi(2)
(1) Japan Aerospace Exploration Agency, Kakuda Space Propulsion Center,
(2) Tohoku University , Department of Aeronautics and Space Engineering

Keywords: Scramjet, Engine performance, Thrust

Abstract: Thrust performances of scramjet engines were compared with theoretical values to quantify the progress in engine performances from Mach (termed as "M") 4 to M8 flight conditions. An engine with a ramp produced a net thrust of 215 N under the M8 tests and a comparison of a theoretical thrust yielded a thrust achievement factor of 51%. By excluding boundary layer, an engine with a thick strut delivered a net thrust of 560 N and showed a thrust factor of 92% and a net thrust factor of 45%. The thrusts were limited by flow separation caused by engine combustion (termed as "engine unstart"). The starting characteristics was improved by boundary layer controls in M6 and M4 conditions. An engine with a thin strut doubled the thrust from 1620 N to 2460 N by the boundary layer bleeding in the M6 tests. The improved thrust factor was 60% at the stoichiometric H_2 condition. Under M4 tests, the net thrust was tripled by the bleed and a two-staged injection of H_2. As results, the thrust factor was raised from 53% to 70%, the net thrust factor was increased from 32% to 55%. Studies required for improving the net performance was addressed.

Nomenclature

A_1	Inlet area （0.2 m-wide×0.25 m-high)
cf	wall friction coefficient
Cint	Internal drag coefficient of engines
Dint	Internal drag of engines （= Cint·q_1·A_1)
Df	Internal friction drag on engines
Df0	Minimum friction drag on the internal surface of a rectangular duct
Dp	Internal pressure drag of engines
d1	Displacement thickness of boundary layer
Isp	Fuel specific impulse (km/s)
M	Mach number
q_1	Freestream dynamic pressure at inlet (kPa)
□p	Total pressure recovery factor
□c	Air capture ratio in inlets
□F	Thrust increment by combustion
□Fnet	Net thrust by combustion (= □F - Dint)
□drag	Drag achievement factor (= Df0/Dint)
□□F	Thrust achievement factor (= □Fexp /□F0)
□net	Net thrust achievement factor
□	Geometrical contraction ratio of inlets
□	H_2 equivalence ratio

subscripts

exp	experimental values
0	baseline values

Introduction

Development of hydrogen (H_2)-fueled scramjet engines is being undertaken under flight conditions of Mach 4, 6 and 8 at Japan Aerospace Exploration Agency. In the engine tests, our engines delivered net thrusts which overcame the engine drag. However, the thrust was limited by the occurrence of inlet unstart (termed "engine unstart" or simply "unstart") due to combustion. It is caused by the boundary layer separation in inlets of engines. Therefore, boundary layer bleeding and two-staged injection of H_2 were examined to extend the engine operational range to □1. Details of our previous work, the facility employed and the engine testing are described in Ref. 1, and recent progress can be found in Refs. 2 to 6.

This paper has four objectives;

1) Examinations of accuracy of our thrust measurements
2) Reviews of our M4 to M8 engine performance
3) Quantification of the thrust, net thrust performances achieved in our engine tests,
4) Drag reduction for improving the net performance.

Two thrust measurements, namely one by a force measerement system (FMS) and the other by wall pressure integration are explained to facilitate the accuracy of our engine testing. Engine data about the thrusts and the specific impulse are reviewed in the M4, M6 and M8 conditions. To improve engine performance, it is necessary to compare the engine data with values obtained theoretically. Therefore, fast fuel mixing and combustion distributed downstream of the engine throat are assumed to calculate the theoretical performance.[7] Comparison of the engine data with the theoretical values enables quantification of the engine performances achieved under Mach 4, 6 and 8 flight conditions. These performances with regards to combustion, net thrust and engine drag are discussed.

Engine Geometry and Analysis

H_2-fueled Scramjet Engines and Test Conditions

Two side-compression-type scramjet engines were constructed in our testing. These engines can be quickly and easily reconfigured so that various struts and ramps in the engines can be tested. The engines are all rectangular and consist of a cowl, a top wall and two sidewalls (Fig. 1). The entrance and the exit of the engine are 200 mm wide, 250 mm high (denoted by H) and 2.1 m long. The inlet is a sidewall compression type with a 6-degree half angle. The engines have a swept-back angle of 45 degrees to deflect the airstream for suitable spillage required in inlet starting. The baseline engine has the swept back angle throughout the engine (named E1 engine). The

geometrical contraction ratio is 2.86 without struts. Inlets with struts and ramps were tested to examine the inlet and combustion performances.[1]

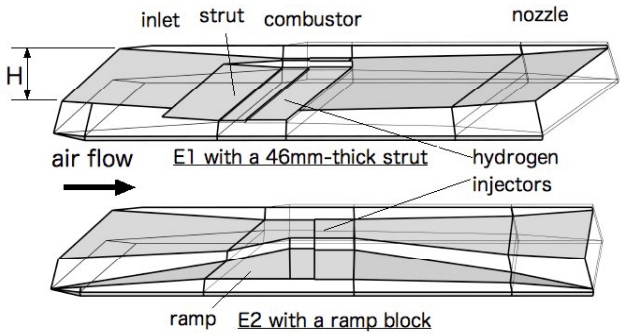

Fig. 1 Engine with a strut (E1) and with a ramp (E2)

Since severe distortions of air and H_2 flows were detected by gas sampling in the E1 engines, a new engine (named E2 engine), which is illustrated in the lower part in Fig. 1, was constructed.[2] The swept-back angle is eliminated downstream of the isolator in order to minimize the distortion of the airflow. In some M8 tests, a 1.23-m long, 250-mm high, 46-mm thick strut was installed in the combustor and diverging section (the geometrical compression ratio is 8.3). Instead of the strut, a compression ramp with a compression ratio of 7.94 was also tested. This engine is cooled by sparsely-distributed water channels so that precise measurements of distributions of wall pressure and heating rate are possible. The E1 and E2 engines were tested in the Mach 8 tests, while in the Mach 4 and 6 tests, only the E1 engine was employed.

The test conditions and summaries of engine performances are presented in Table 1, where the inlet Mach number (M1), the displacement thickness of the ingested boundary layer (d_1 in mm), the geometric contraction ratio ( ) and the air capture ratio (c) are shown. The lower Mach numbers represent the engine inlet conditions behind the bow shock of the vehicles. The engines are mounted in a test cell so as to ingest the facility nozzle boundary layer which simulates the effects of vehicle forebody boundary layer ingestion in flight.

The mass rate (Ma in kg/s) of air passing through the inlet is dependent on the boundary layer swallowed by the engines. For example, the air mass rate in the engines with the 5/5H strut is 1.29 kg/s with boundary layer ingestion in the M8 condition, and the mass flow rate increases to 1.48 kg/s by excluding the boundary layer. Boundary layer exclusion was achieved by moving the engine to the core region of the facility nozzle. Since engines easily fell into the unstart due to combustion, the effects of boundary layer bleeding were investigated in the M6 and M4 tests. In the M4 tests, the mass rate of air flowing into the inlet is the same (6.7 kg/s). However, the air flow rate in the combustor decreases by 0.2 kg/s in Table 1. The bleed-air rate in the M6 test is small so that the air flow rate to combustor is unchanged (5.0 kg/s)

The stoichiometric H_2 rate in Table 1 is determined by the air flow rates and found to be from 42 g/s (M8-strut engine) to 195 g/s (M4-strutless engine). The H_2 was injected normally from the sidewalls through 24 fuel orifices in the combustor. In some Mach 4 tests, two-staged injection of H_2 was examined to improve the thrust performance where the additional H_2 was injected at 558 mm downstream of the combustor step.

Internal drag (Dint) of the engines and minimum friction drag of rectangular ducts (Df0) are listed in Table 1. Thrust produced by combustion in engine tests (Fexp), i.e., the axial force of the engine with combustion minus the axial force on engine with no fuel injection (called *air-drag,* Dair), is a key performance. The counterparts estimated by one-dimensional analysis (F1D) are shown for the tested H_2 equivalence ratio ( ). Definitions of the F, net thrust, performance achievement factors of thrust (F), net thrust (net) and drag (drag) are discussed later.

Thrust Measured by a Balance and wall pressure

In our facility, forces acting on engines were measured by a balance (Force Measuring System, FMS) consisting of a floating frame supported by a thrust load-cell and three load-cells for lift and pitching moment. The FMS contains a calibration system and can revise the calibration matrix under conditions of installation of fuel and cooling water supply lines and measurement cables. This FMS measurement is a steady-state measurement in which test conditions are maintained from two seconds to ten seconds for each H_2 rate.

Combustion performance is indicated by a thrust increment measured from the Dair and the increment is termed *thrust by combustion* or simply *thrust* (F) here. The Dair consists of two drags, namely *internal drags* (Dint) worked on the internal walls in engines and *external drags* on the external surfaces. The external drag de-

Table 1 Test conditions, thrust measured and achievement factors of engine performances

	M1	d1		c	Ma	m)H2	Dint	Df0		F1D	Fexp	Fnet	Isp)f	F	net	drag
unit	-	mm	-	-	kg/s	g/s	N	N	-	N	N	N	km/s	-	-	-
M8(5/5H-strut)	6.7	32.8	8.33	0.74	1.29	41.6	660	90	0.42	429	316	-344	-	0.74	-	0.14
(5/5H-strut, w/oBL)	6.7	0	8.33	0.74	1.48	47.9	660	90	2.1	1325	1220	560	5.6	0.92	0.45	0.14
M8 (ramp)	6.7	32.8	7.94	0.80	1.39	44.9	295	90	1.20	1009	510	215	4.0	0.51	0.23	0.31
(ramp-w/o BL)	6.7	0	7.94	0.80	1.6	51.7	295	90	1.3	1200	760	465	6.9	0.63	0.42	0.31
M6(5/5H-strut)	5.3	19.7	5.00	0.80	5.00	145	784	270	0.48	2530	1620	836	12.0	0.64	0.37	0.34
0.6%-bleed	5.3	19.7	5.00	0.80	5.00	145	784	270	1.00	4070	2460	1676	11.6	0.60	0.44	0.34
M4 (w/o strut)	3.4	11.7	2.86	0.72	6.70	195	570	280	0.30	2250	1200	630	10.8	0.53	0.32	0.49
3%-bleed & 2nd H2	3.4	11.7	2.86	0.72	6.50	195	700	280	0.95	3660	2560	1860	10.0	0.70	0.55	0.40

pends on the external geometry and decreases when engine modules are clustered. On the other hand, the Dint is related to irreversible processes, such as spill drag and total pressure loss in engines. It is the most important, intrinsic property for evaluating engine performance. Therefore, *net thrust* is defined as F - Dint.

The air-drag measured by the FMS includes the external drag in addition to the Dint. Mitani et al. have proposed a method to evaluate the pressure drag (Dp) and the friction drag (Df) on internal walls of engines based on wall pressure measurements[8] and examined its accuracy in various engine geometries and flight conditions.[9]

In order to examine accuracy in the F measured by the FMS, the F was also evaluated by integration of engine wall pressure (Pw). Correlation between these two measurements is plotted in Fig. 2. The data symbols denote different test conditions. All the data were correlated by Y = 1.03X – 176N. Considering experimental errors (+-100 N) including repeatabilities of engine tests, the discrepancy of 3% in the slope is within the errors. Thus, Figure 2 indicates the reliability and accuracies of the two, independent thrust measurements.

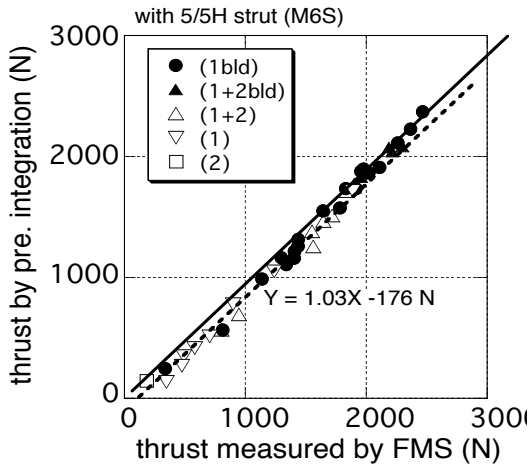

Fig. 2 Correlation between F by FMS and wall pressure

Quantification of Achieved Performances

The flow field is supersonic in scramjet engines and the flow upstream of the combustors is not affected by combustion. Therefore, thrust delivered in expansion sections downstream of the combustor can be calculated by any reactive flow calculations. In this study, our two in-house codes assuming chemical equilibrium flow were used and effects of quenching of dissociated species in low-pressure flow were investigated by a one-dimensional reactive flow code.[8] The upstream boundary conditions at the engine throat were evaluated from experimental data from the subscaled wind tunnel.[6,7] The increment of thrust from the value under the airflow condition corresponds to the F obtained in engine tests. Experimental values (Fexp in N), theoretical values (F1D), corresponding H_2 flow rates ( ) and fuel specifiulses (Isp in km/s) are summarized in Table 1.

Since the total pressure loss by heating (Rayleigh loss) becomes significant and dependent on combustion in engines, theoretically-available thrusts are not uniquely defined. As a result, the combustion schedule must be specified to calculate the performance. Concentrated combustion at the engine throat yields the maximum thrust if the supersonic condition is satisfied in engine flow. However, this high combustion rate easily causes thermal choking in engines operating at lower Mach numbers. In addition, this thermal choking also restricts the operation in engines in high Mach number flights, because these engines require higher compression ratios for combustion (then a lower M in the combustor).

In order to evaluate the maximum thrust as baseline data, the F1D was calculated under two assumptions: an infinitely fast mixing of fuel by the combustor entrance and a distributed combustion downstream of the throat in which the combustion proceeded with M = 1 being maintained in the diverging section.[7] This *distributed combustion* minimizes the Rayleigh loss and avoids the thermal choking in supersonic combustion engines.

Achievement Factors of Engine Performance

In order to evaluate how high or low our engine performances are, the achievement factors of combustion and net thrust are quantified. The thrust achievement factor (F) is defined by comparing the experimental thrust with the one-dimensional thrust. This reflects the combustion performance in engines.

$$\eta_F = F_{exp} / F_{1D} \quad (1)$$

Although F represents the combustion performance of the engine, it does not directly indicate the net performance of engines. For instance, a large flameholder in combustors enhances combustion. However, the large flameholder increases the engine drag, resulting in loss of thrust propelling vehicles. Net thrust is defined by the thrust increment by combustion minus the internal drag. For a net thrust achievement factor (net), the numerator is evaluated based on the experimental thrust and the measured internal drag. The denominator giving the maximum net thrust is defined by using the one-dimensional thrust and a minimum internal drag (Df0).

$$\eta_{net} = (F_{exp} - D_{int}) / (F_{1D} - Df_0) \quad (2)$$

The minimum drag is evaluated using an ideal engine consisting of four flat plates, the drag of which is only friction. All the waves are canceled out in the ideal engine such that no pressure drag exists. The details will be discussed in a later section.

Performance Attained in Engine Tests

Mach 8 Condition

Engines with struts and a ramp

Figure 3 presents the F1D and Fexp measured in the engine with the 46-mm-thick strut.[2] The c and the p necessary for the calculations were measured in subscaled wind tunnel tests. One-dimensional analysis indicates that thrust increases with the and thermal choking oc-

curs near □ = 1 if H_2 fuel completely burns at the throat. The distributed combustion yields a thrust of 880 N at □1 and shows increasing thrust beyond □1 due to mass addition and molecular weight reduction by H_2.

Engine data for various engine configurations are plotted in Fig. 3. The solid data denote results obtained from the E2 engine and the open symbols are for the E1 engine. The solid circles for the engine with the large 46-mm thick strut show the highest combustion performance close to the theoretical line at a given □. However, the engine fall into inlet unstart after attaining the maximum thrust of 316 N at □0.42. A maximum thrust of 425 N at □1.4 is observed in the E1 engine with a 46-mm-thick, 637-mm-long strut (open diamonds).

Engine thrust varies depending on the strut geometries and H_2 injection patterns. When a 1229-mm-long strut is installed (solid triangles), the thrust increases. However, the engine easily fall to the unstart condition at □ = 0.6. When H_2 is concentratedly injected near the cowl, combustion deteriorates (solid squares). Generally speaking, larger struts enhance combustion and the resulting better combustion performance promotes the inlet unstart. If the performances are evaluated using the best □Fexp (316 N at □0.42) of the solid circle and the corresponding □F1D (429 N), the □□F is 74%.

The Dint (660 N) of the E2 engine with the 46-mm-thick strut is also indicated by the horizontal line. If this drag is subtracted from the best □Fexp of 316 N, the □Fnet for the solid circle becomes a negative value of -344 N. Although the engine with large strut shows the better combustion performance, the large strut increases Dint resulting in loss of □Fnet. For engines with struts, it is necessary to reduce the Dint and to extend the engine operation range to □1.

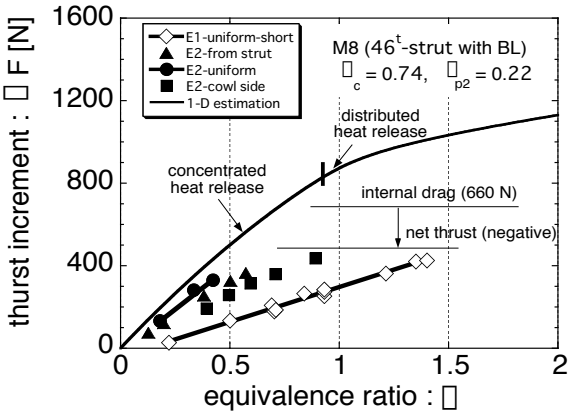

Fig. 3 Measured thrusts and the comparison with analytical value (M8-46-mm thick strut engine)

Thrust and drag performances in the engine with a ramp were measured under the M8.[3] Thrusts of 932 N at □1 and of 1009 N at the thermal-choking limit were attained with concentrated combustion at the throat. Measured thrust increased proportional to the fuel supply and reached the maximum □Fexp of 510 N at □1.2. Then it decreased in □ >1.2. Evaluation at □1.2 yielded □Fexp = 510 N and □F1D = 1009 N, and the □□F was 51%.

As shown in Table 1, the Dint of the ramped engine was small, i.e., 295 N. Consequently, the maximum □Fnet was found to be 215 N at □1.2. The theoretical □Fnet was evaluated to be 915 N from the minimum drag of 90 N. Comparison of two □Fnet yielded a □net of 23%. The positive □Fnet in the ramp engine was due to the small Dint and the extension of the operational range to □1.2.

However, the net thrust performance is not sufficient. Table 1 indicates that the net Isp is about 4 km/s. The lower □□F of 51% implies that the combustion efficiency must be doubled. The □net of 23% suggests that the specific impulse may be raised to 17 km/s by improvement of the combustion performance and the drag performance.

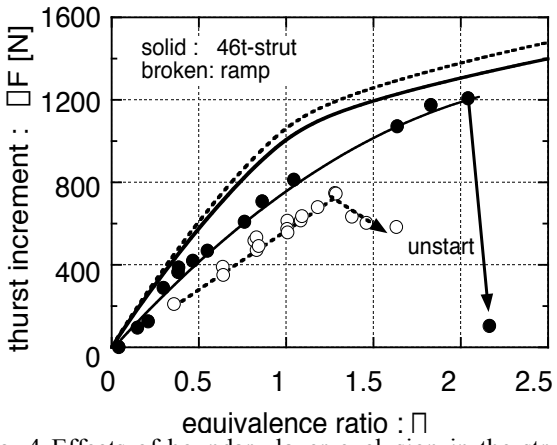

Fig. 4 Effects of boundary-layer exclusion in the strutted and ramped engines (M8)

Effects of Boundary Layer Ingestion

Effects of swallowing of the boundary layer by engines were examined by moving the engines into the core flow in the facility nozzle in the M8 testing.[4] Figure 4 summarizes the engine data and the theoretical performances, the solid lines denoting the □F by the engine with the 46-mm-thick strut and the broken lines denoting □F in the ramp engine. The airflow rate in the engines increases by 15% as shown in Table 1 when the engines are moved into the core region of the facility nozzle. Therefore, the thrust by the engine excluding the boundary layer increases by 15% at a given □. The reason why the □F1D by the engines with the strut in Fig. 4 are greater than that in Fig. 3 is due to this increase of their mass flow rates. Similarly, the reason that the □F1D by the strut engine is lower than that by the ramp engine is the lower □c in the strut engine (Table 1). The subscale wind testing confirmed that the moving of engine into the core flow had negligible effects on the □p and the Dint of engines.[7]

When the engine with the 46-mm-thick strut swallowed the boundary layer on the facility nozzle, it fell into inlet unstart at □0.4 as shown in Fig. 3. However, the solid circles in Fig. 4 indicate that the engine operates up to □2.1 when the boundary layer is excluded. The maximum □Fexp measured is 1220 N and the □□F is found to be 92% by comparison with the □F1D of 1330 N at □2.1. With exclusion of the boundary layer, the strut engine can produce a □Fnet of 560 N and the □net is 45%. In the ramp engine, the operational range was extended from □1.2 to □1.3 and the maximum □Fexp increased from 510 N to 760 N and the □Fnet was doubled to 465 N.

Mach 6 Condition

The test data in the M6 condition was illustrated in Fig. 5.[6] In these experiments, a 30-mm-thick strut was installed in the engine. The combustion switches from a weak mode (flame blown-off to the downstream section) to an intense mode (flame anchored in the combustor) and causes a jump in thrust near □0.3. Above □0.3, engine operates in the intense combustion mode and exhibits a hysteresis between two combustion modes. When the boundary layer was not bled, the engine fell into the unstart at □0.48 just after attaining the maximum thrust of 1620 N. Thus the limit fuel rate in the baseline engine was □0.48 without the bleed.

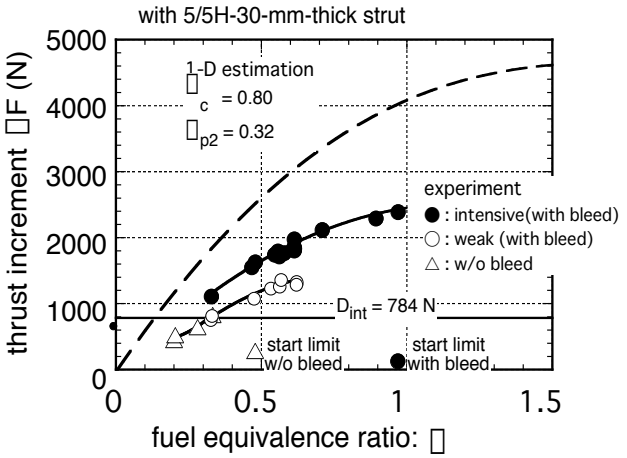

Fig. 5 Measured thrusts and the comparison with analytical value (M6-struted E1 engine)

Figure 5 shows that the bleed of 30 g/s (0.6% of captured air in the engine) extends the start limit from □0.48 to □1 to deliver the maximum thrust of 2460 N. The Dint of 784 N, the □Fnet is 1676 N and the fuel Isp is calculated to be 11.6 km/s as shown Table 1. The achievement factors of the thrust and the net thrust was evaluated by comparisons with analysis. In Figure 5, the theoretical curve is estimated by assuming the distributed combustion in □ > 0.4. Since the □F1D at □1 is 4070 N as indicated in Table 1, the □□F and □net become 60% and 44%, respectively. These achievement factors suggest that the Isp may be raised to 19.3 km/s by improving the combustion performance and to 26 km/s by improving the drag performance of the engine in addition to the combustion.

Mach 4 Condition

Figure 6 shows a comparison of □F1D and □Fexp measured in the engine with neither struts nor ramp (□ = 2.8).[5] Because the incoming flow Mach number is as low as 3.4, the engine is easily thermally-choked at □0.1 if concentrated combustion at the throat is assumed. Therefore, the distributed M1 combustion in the downstream section of the engines is assumed in □ > 0.1 in Fig. 6. The □F1D increases from 2250 N at □0.3 to 3650 N at □1. With increasing □, the combustion region is moved down to the engine exit and the high pressure area generating thrust is confined to the narrow section near the nozzle. The saturated behavior in the □F1D in Fig. 6 is attributed to this limited thrust surface.

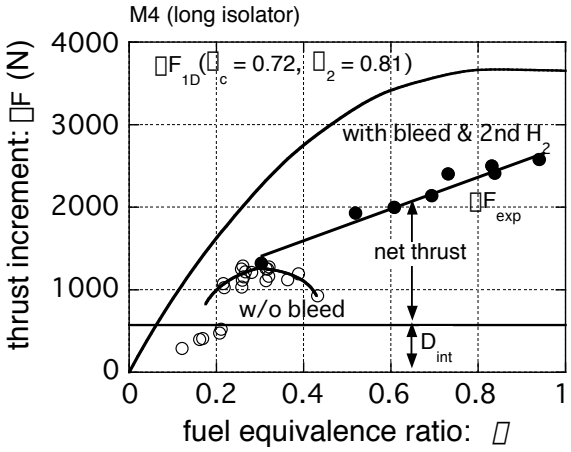

Fig. 6 Measured thrusts and the comparison with analytical value (M4-E1 engine without strut)

The open symbols in Fig. 6 denote baseline data obtained in the engine and the solid symbols are for the engine with boundary layer bleed and two-staged injection of H_2. The switching of combustion modes is observed at □0.2 at which the □Fexp jumps from 500 N to 1000 N. The engine without bleed attains a maximum □Fexp of 1200 N at □0.3 and the □Fexp gradually diminishes □ > 0.3. This diminished □Fexp is caused by the intrusion of high pressure into the inlet. Since the Dint of the baseline engine is 570 N (Table 1), the □Fnet is 630 N and the Isp is 10.8 km/s. The □□F and □net are 53% and 32%, respectively, where the Df0 is evaluated to be 280 N.

There are two reasons for this poor □net in the engine. The first is the large Dp in the internal drag. As discussed later, the Df is near the lowest limit and it is difficult to further decrease it. The spillage drag governs the Dp at the lower Mach number and must be optimized in the engine. The second reason is that the start range is restricted to less than □0.3 leading to a small thrust value. To increase the thrust it is necessary to raise the wall

pressure near the engine throat and utilize the thrust surface effectively. However, a pressure increase near the throat causes intrusion of separation into the inlet and promotes the unstart. If the boundary layer is controlled, the poor net of 32% is greatly improved.

Two methods were tested in the Mach 4 engine, namely the boundary layer bleed and the two-stage injection of H_2. A porous plate was installed which extended from the exit of the inlet to the isolator section on the topwall. Suctioned air of 200 g/s (3% of engine airflow) was metered by an orifice in the bleed device and exhausted to the test cell. Tomioka et al reported that two-stage injection was effective for moderating of the pressure rise in the combustor and retarding the inlet unstart.[10] In engine tests, the second injectors were located 558 mm downstream of the step in the combustor (462 mm upstream of the engine exit). The second H_2 was perpendicularly injected from orifices on the sidewalls.[5]

Effects of the bleed and the second injection are shown by the solid symbols in Fig. 6, where the engine operates up to 0.95 and the maximum Fexp increases from 1200 N to 2560 N. Although bleed of 200 g/s increased the Dint from 570 N to 700 N, the Fnet was improved from 630 N to 1860 N. The Isp is found to be 10 km/s. This Isp lower than the Isp (10.8 km/s at 0.3) in the baseline engine is attributed to two factors: the thrust data near 1 and the poor combustion efficiency of the secondarily-injected H_2. The maximum Isp resulting from the bleed without the second injection was found to be 12.4 km/s at 0.66.

Table 1 shows that the F is improved from 53% to 70% and that the net becomes from 32% to 55% as the result of bleeding and the two-staged injection of H_2. The combustion efficiency in the lower region is high because the F is 80% at 0.25. It is easy to improve the combustion efficiency of the secondarily-injected H_2 in larger flight-type engines. The mixing and combustion in external nozzles in vehicle aftbodies also promise to result in better combustion because the residence time becomes greater there.

Drag Performance of Engines

The net thrust is governed by the magnitude of the Dint. Figure 7 presents the dependencies of Dint on the flight Mach numbers and the engine geometries.[9] The drag is expressed as drag coefficients defined by using the q_1 and the engine inlet area (A_1). For instance, the column on the far-left shows the breakdown of the Cint in the strutless engine (= 2.86) in the M4 condition. The Cdp and Cdf are 0.061 and 0.054, and their sum yields Cint of 0.115. It was impossible to stabilize combustion in an engine without struts in the M6 flight condition. The flameholding was achieved by a 30-mm-thick, 1/5H-high strut. The 30-mm-thick, 5/5H-high strut further improved the combustion performance as shown in the previous section. However, in Fig. 7, the Cdf is doubled and the Cint is increased to 0.150 by the strut.

The higher Mach number decreases the Cdp in the engine. For instance, when the 30-mm-thick strut is installed in the M8 condition, the Cint becomes 0.133, 80% of it being Cdf. Since the strut was found to be insufficient for the M8 combustion, the 46-mm-thick strut was employed to attain the better combustion performance. This large strut with = 8.33, however, increases the Cdp and Cdf and consequently doubles the Cint coefficient to 0.244. This is the reason why the engine cannot deliver the net thrust as explained in Fig. 3. The column on the far-right shows the Cint breakdown drag of the ramp engine in the M8 condition. Although the engine has an 7.94, nearly equal to that in the engine with the 46-mm strut, the Cint decreases to less than half and is smaller than that with the 30-mm-thick strut (= 5). This is attributed to the reductions in the base drag and the wet surface area of the strut.

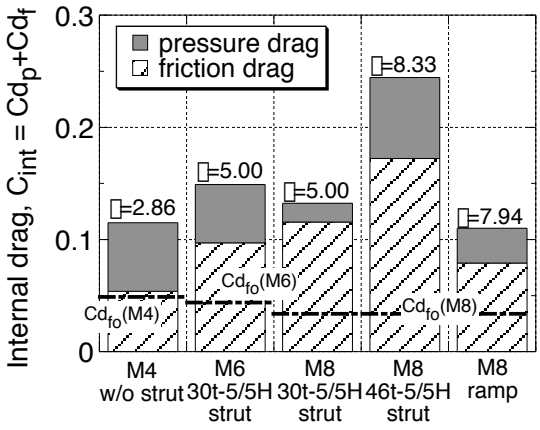

Fig. 7 Breakdowns of friction and pressure drags in the internal drag.

Achievement Factor for Drag Performance

An estimation of the minimum drag is necessary to discuss the magnitudes of the Dint and to quantify the achievement of drag reduction. An ideal engine, which is comprised of an isentropic compression inlet and an isentropic expansion downstream of the throat, is assumed. No pressure drag is produced in the engine. However, there is the friction drag. The minimum friction drag (Df0) can be estimated from an engine duct consisting of four flat plates with geometry similar to that of the engine. The Df0 of the internal walls is calculated for a duct with a width (W), a height (H) and a length (L). The drag is defined as a ratio of the Df0 and the Dint measured in the test engines.

$$\eta_{drag} = Df_0 / D_{int} \quad (3)$$

$$Df_0 = c_f \cdot A_{wet} \cdot q_1 \quad (4)$$

$$c_f = 0.472 (\log Re_L)^{-2.58} \Big/ \left(1 + \frac{\gamma - 1}{2} M_1^2\right)^{0.467} \quad (5)$$

$$A_{wet} = 2(H + W)L \quad (6)$$

The □drag is an indicator of how close the test engines are to the ideal engines with no wave drag.

The □drag is evaluated from the minimum friction drag in Table 1 and Fig. 7. The Cdf0 are indicated by the horizontal, broken lines in Fig. 7. In the M8 condition, the □drag in the engine with the 30-mm thick strut is 0.29 (Table 1). The replacement with the 46-mm-thick strut lowers it to 0.14. This poor □drag causes the negative net thrust in Fig. 3. The large strut has a Cdf of 0.172, which is five times greater than the Cdf0 of 0.038 in the rectangular duct. This large Cdf is caused by the large wet area and the increases of dynamic pressure and the wall friction coefficient. Replacing the strut with the ramp improves a □drag from 0.14 to 0.31, where the Cdf is halved from 0.172 to 0.079 and the Cdp decreases from 0.072 to 0.041.

In the M4 condition, the strutless engine indicates a small Cdf of 0.057, which is comparable to the Cdf0 in the rectangular duct (0.052). This means that the engine is close to the rectangular duct and it is impossible to decrease the Cdf any further. On the other hand, the Cdp is found to be 0.061. The large spillage of air in the inlet in the M4 condition is responsible for the large Cdp. As the result, the □drag is found to be 0.49. The Cint may be halved by minimizing the Cdp. The spill rate and the additive drag produced by the spilled flow have to be optimized in inlet designs to improve the □drag and the □net in lower Mach number flights.

Summary

Baseline thrust performance was estimated by one-dimensional analyses to quantify the thrust, the net thrust and the drag performances attained in our engine tests from Mach 4 to Mach 8. Comparisons with the engine test data lead the following conclusions.

1) The engine with a ramp compression inlet delivered a maximum thrust of 510 N and a net thrust of 215 N in the M8 condition. Comparison with the theoretical thrust and the minimum drag yields thrust and net thrust achievement factors of 51% and 23%, respectively.
2) Exclusion of the boundary layer extended the engine operational range from □0.4 to □2.1 and produced a maximum thrust of 1220 N and a net thrust of 560 N. This improved the thrust and net thrust factor to 92% and 45%, respectively.
3) The baseline engine with a 30-mm-thick, 5/5 H-high strut showed a thrus of 1620 N under the M6 condition. The thrust and net thrust factors were 63% and 45% in the engine without the boundary layer controls.
4) The engine without struts in the M4 condition operated with distributed combustion in □ > 0.1. The thrust factor was 53% and the net thrust factor was as low as 32% due to the large pressure drag. The pressure drag should be minimized by optimizing the spillage of the inlet in lower Mach number flights.
5) The boundary layer bleed of 3% air and the two-stage combustion in the M4 condition increased the thrust threefold and attained a maximum net thrust of 1860 N (Isp = 10 km/s). The thrust and the net thrust achievement factors were evaluated to be 70% and 55%. Under the M6 condition, the 0.6% bleed increased the thrust from 1620 N to 2460 N and doubled the net thrust.

Reference

[1] Chinzei, N., Mitani, T. and Yatsuyanagi, Y., "Scramjet Engine Research at the National Aerospace Laboratory in Japan," Scramjet Propulsion, edited by Curran, E. T. and Murthy, S. N. B., Vol. 189, Progress in Astronautics and Aeronautics, AIAA, New York, 2001, pp159-222.

[2] Kobayashi, K., Tomioka, S., Kanda, T., Tani, T., Hiraiwa, T., and Saito, T., Modified Water-cooled Scramjet Engine Tested under M8 Condition, AIAA Paper 2001-3202, (2001).

[3] Hiraiwa, T., Kanda, T., Mitani, T. and Enomoto, Y., "Experiments on a Scramjet Engine with Ramp-Compression Inlet at Mach 8 condition," AIAA Paper 2002-4129, presented at the 38th Joint Prop. Conf., Indianapolis, 2002.

[4] Hiraiwa, T., Kanda, T., Kodera, M., Saito, T., Kobayashi, K., Kato, T., Effect of Induced Boundary Layer on Scramjet Engines' Thrust and Combustion Characteristics, AIAA 2003-4739, presented at 39th Joint Prop. Conf.,(2003).

[5] K. Kobayashi, S. Tomioka, T. Hiraiwa, K. Kato, T. Kanda, and T. Mitani, "Suppression of Combustor-Inlet Interaction in a Scramjet Engine under M4 Flight Condition," AIAA 2003-4737, presented at 39th Joint Prop. Conf., (2003).

[6] Kodera, M., Tomioka, S., Kanda, T. and Mitani, T., Mach 6 Test of a Scramjet Engine with Boundary-Layer Bleeding and Two-Staged Fuel Injection, to be presented at the 12th Spaceplane Conference, Norfolk, 2003.

[7] Kouchi, T., Mitani, T., Hiraiwa, T., Tomioka, S., Masuya, G., Evaluation of Thrust Performance in Kinetic-Controlled Scramjet Engines with Measured Internal Drag, submitted to Journal of the Japan Society for Aeronautical and Space Science, 2003 (in Japanese).

[8] Mitani, T., Hiraiwa, T., Tarukawa, Y., and Masuya, G., Drag and Total Pressure Distributions in Scramjet Engines at Mach 8 Flight, Journal of Propulsion and Power, Vol.18, No.4, (2002), pp.953-960.

[9] Mitani, T., Izumikawa, M., Watanabe, S., Tarukawa, Y., Force Measurements of Fixied Geometry Scramjet Engines from Mach 4 to 8 Flight Condition, AIAA2002-5351, 2002.

[10] Tomioka, S., Murakami, A., Kudo, K. and Mitani, T., Combustion Tests of a Staged Supersonic Combustor with a Strut, J. Prop. and Power, vol. 17, No. 2. pp293-300, 2001.